Scale Dependence of Biogeochemical Reaction Rates: Experimental and Modeling Approaches

Carl I. Steefel
Li Li
Li Yang

Lawrence Berkeley National Laboratory

Origin of Discrepancy between Laboratory and Field Rates

- **Discrepancy between laboratory and field rates may be 3 to 5 orders of magnitude**

- **Possible explanations**
  - ↗ **Passivation of mineral surfaces with time (White and Brantley, 2003; Maher et al., 2004)**
  - ↗ **Slowing of rates close to equilibrium (the "affinity effect")**
  - ↗ **Physical heterogeneity (Malmstrom et al., 2000)**
  - ↗ **Geochemical heterogeneity (Li et al., 2006)**
  - ↗ **Microbiological heterogeneity (????????)**

- **Might some part of the discrepancy be due to the scale dependence of rates in the subsurface?**
  - ↗ **If so, at what scales (pore to pore network to meter) does this scale dependence arise?**
  - ↗ **Some studies without physical/chemical heterogeneity have shown a discrepancy (Maher et al, 2006), so this cannot explain 100%**

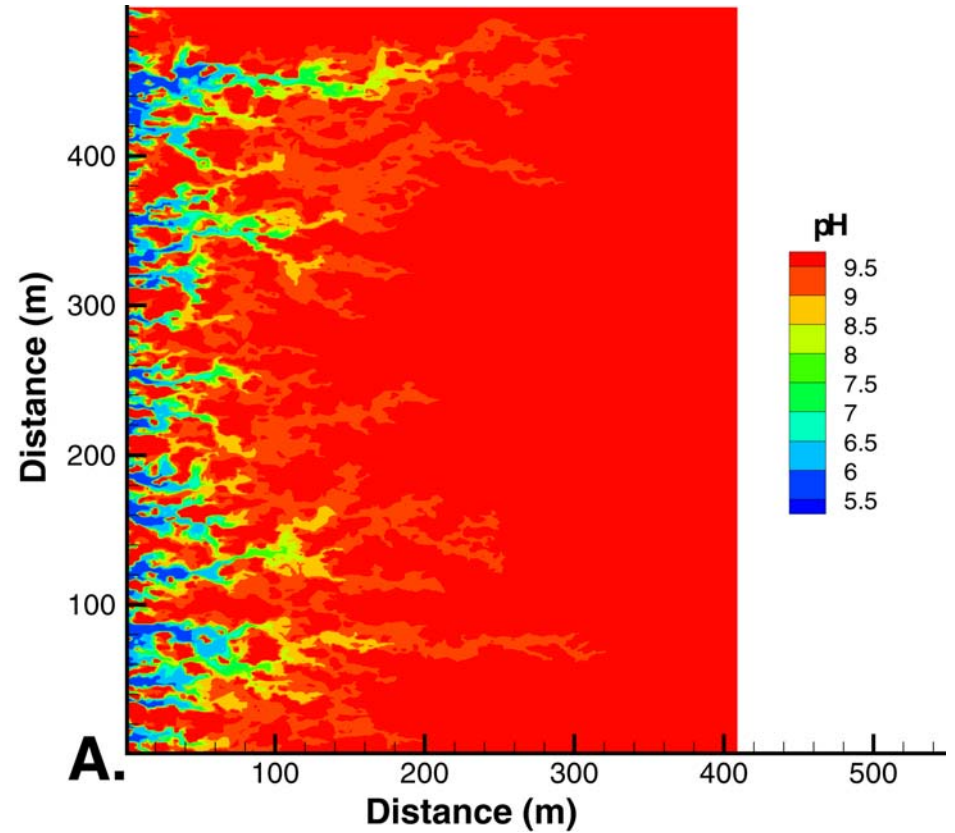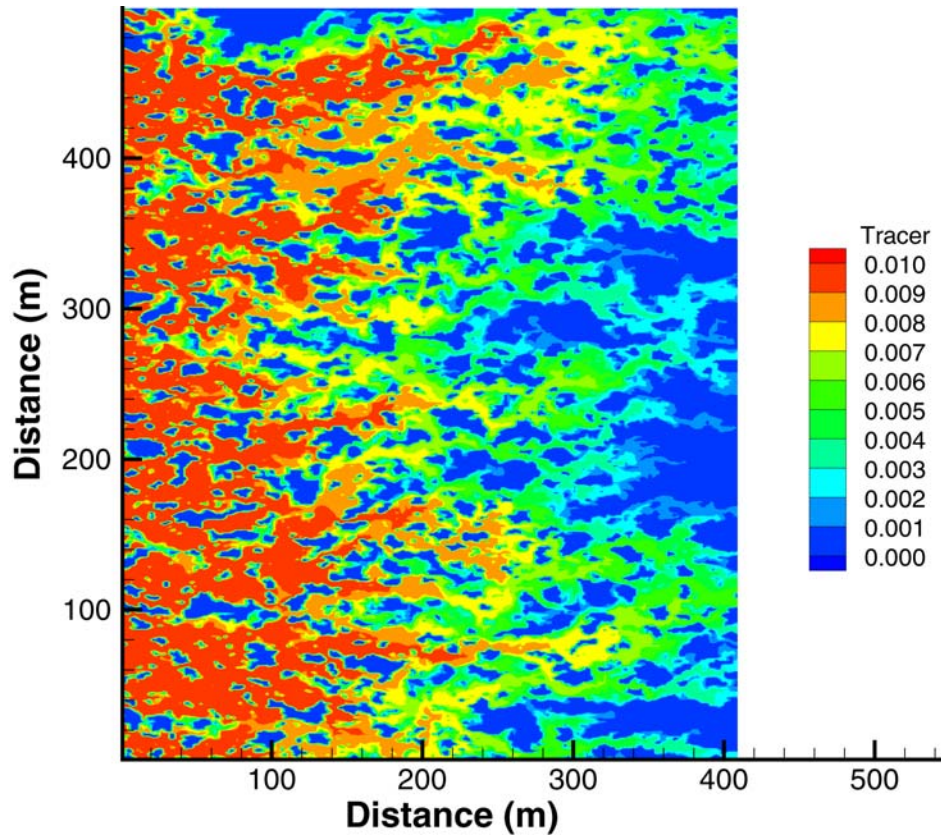# Role of Physical Heterogeneity
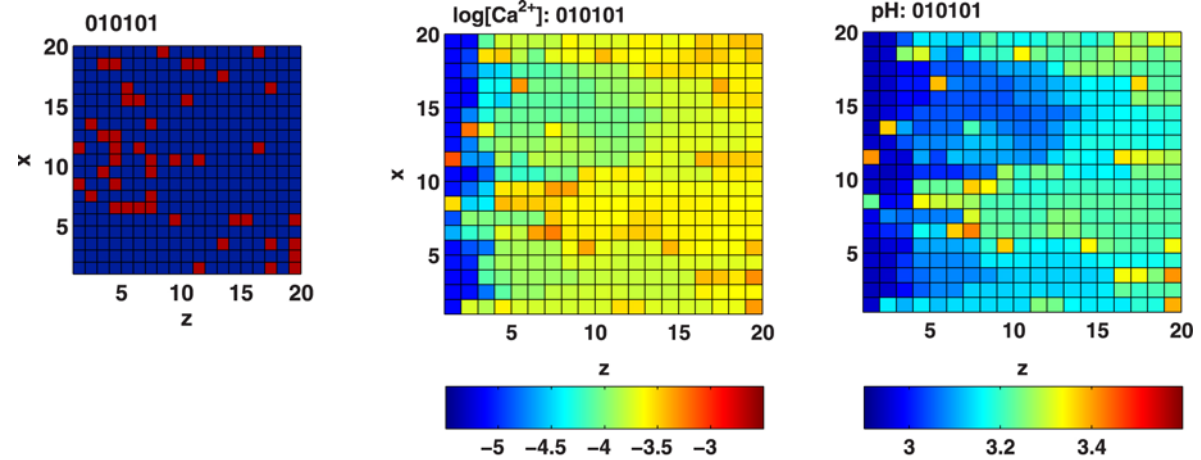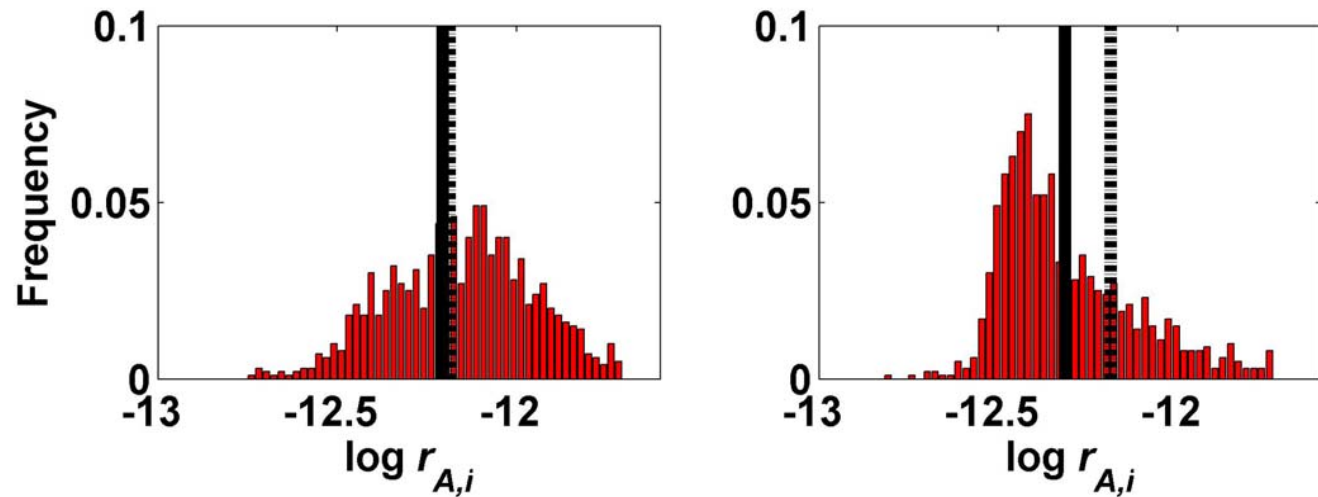

Flow Direction

Non-reactive tracer

pH

Role of Geochemical Heterogeneity

Heterogeneous
distribution of plagioclase
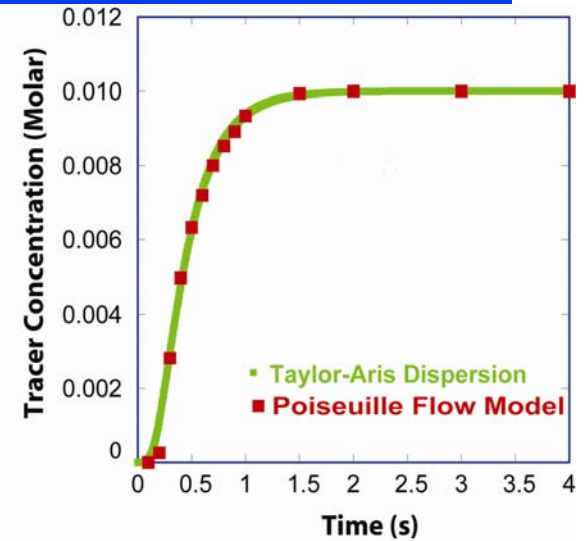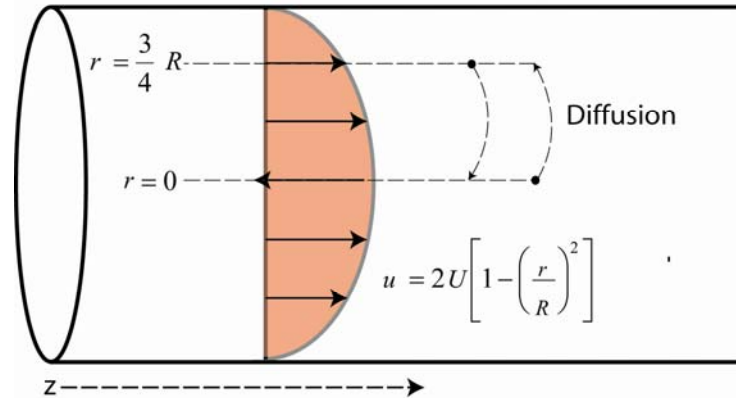at the pore network scale
(Li et al., 2007)

Distribution of
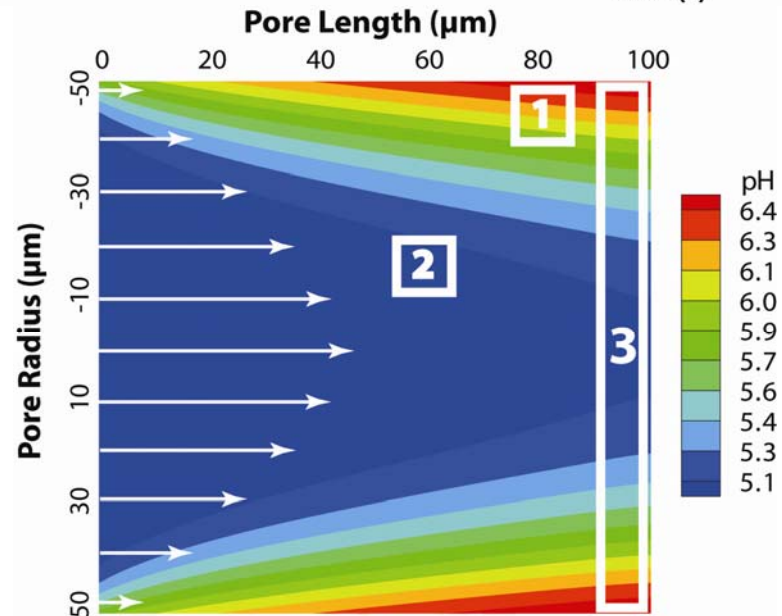reaction rates within
pore network

Does A Scale Dependence Occur at the Pore Scale?

Conceptual model for cylindrical pore

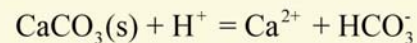Reaction rate that is measured depends on the scale of the measurement

Scaling in the Context of "Realistic" Rate Laws

Calcite Dissolution

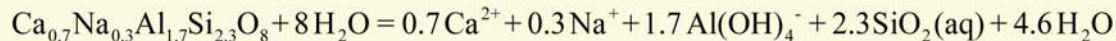One of the most important and fastest mineral reactions in the subsurface.

$$CaCO_3(s) + H^+ = Ca^{2+} + HCO_3^-$$

$$R = A\, a_{H^+} \left[1 - \left(Q \Big/ K_{eq} \right) \right]$$

The reaction rate depends on pH under acidic conditions.

Plagioclase Dissolution

An example of slow silicate dissolution.

$$Ca_{0.7}Na_{0.3}Al_{1.7}Si_{2.3}O_8 + 8\,H_2O = 0.7\,Ca^{2+} + 0.3\,Na^+ + 1.7\,Al(OH)_4^- + 2.3\,SiO_2(aq) + 4.6\,H_2O$$

Hellmann Rate Law
(Hellmann and Tisserand, 2006)

The reaction rate depends on pH and reaction affinity.

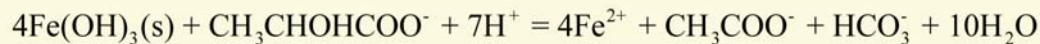$$R = A\, a_{H^+}^{0.7} \left[1 - \exp\left(n \Delta_G^{m1} \right) \right]^{m2}$$

Aluminum inhibition (Oelkers) rate law

$$R = k \left(\frac{K_f'}{a_{Al(OH)_3}^{1/3} + K_f'} \right) \left(1 - \left(\frac{Q}{K_{eq}} \right)^{1/3} \right)$$

The reaction rate depends on pH and dissolved aluminum.

Dissimilatory Iron Reduction

One of the most important biogeochemical reactions.

$$4Fe(OH)_3(s) + CH_3CHOHCOO^- + 7H^+ = 4Fe^{2+} + CH_3COO^- + HCO_3^- + 10H_2O$$

Monod rate law

$$R = \mu_{max} B \left[\frac{C_{Fe(OH)_3}}{K_{Fe(OH)_3} + C_{Fe(OH)_3}} \right] \left[\frac{C_{Lactate}}{K_{Lactate} + C_{Lactate}} \right]$$

A

Calcite sample
(4000 micron thickness)

Supporting ceramics
(100 micron thickness)

500 micron
diameter hole

B

Legend:
- Experiment, pH = 5
- Modeling, pH = 5
- Experiment, pH = 4
- Modeling, pH = 4

Y-axis: Ca²⁺ Concentration (µMolar)

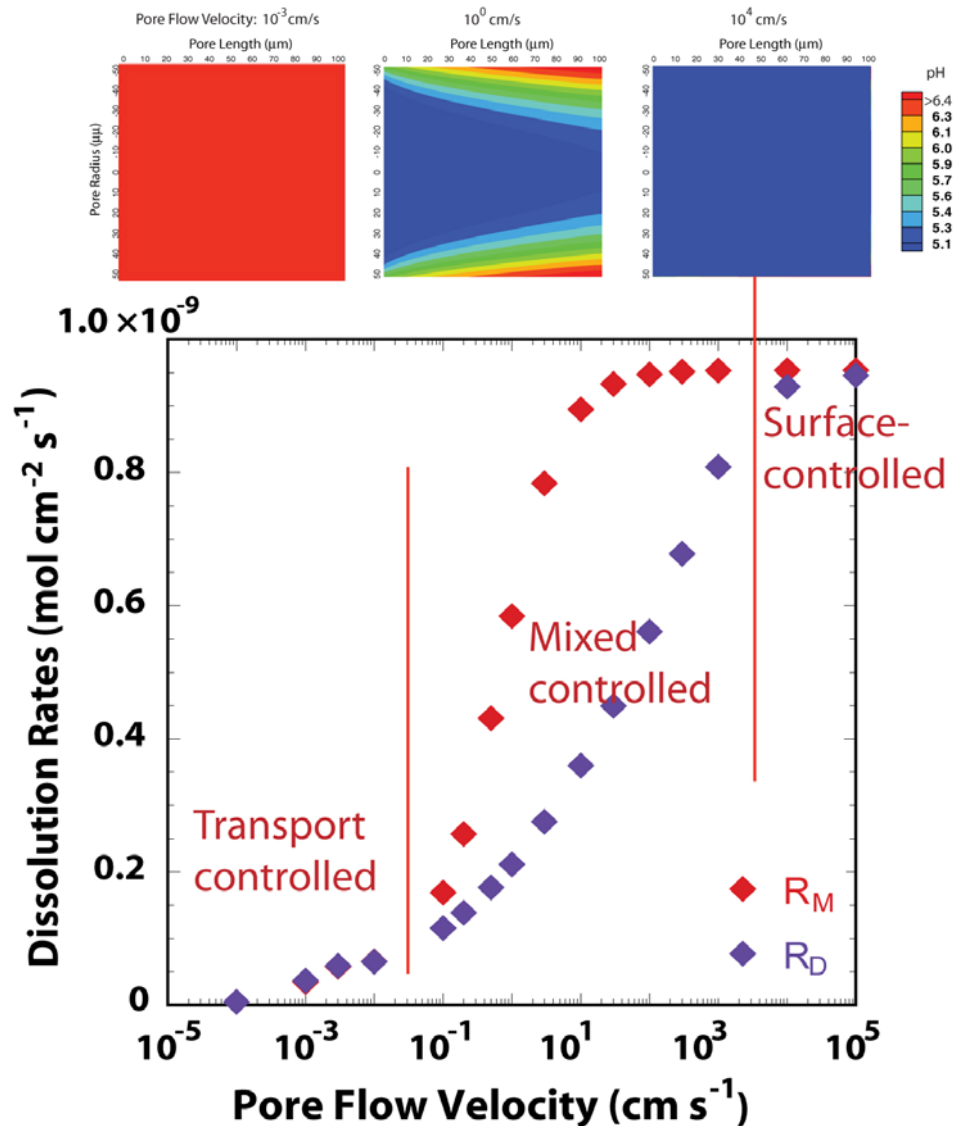X-axis: Flow rate (µLiters/min)
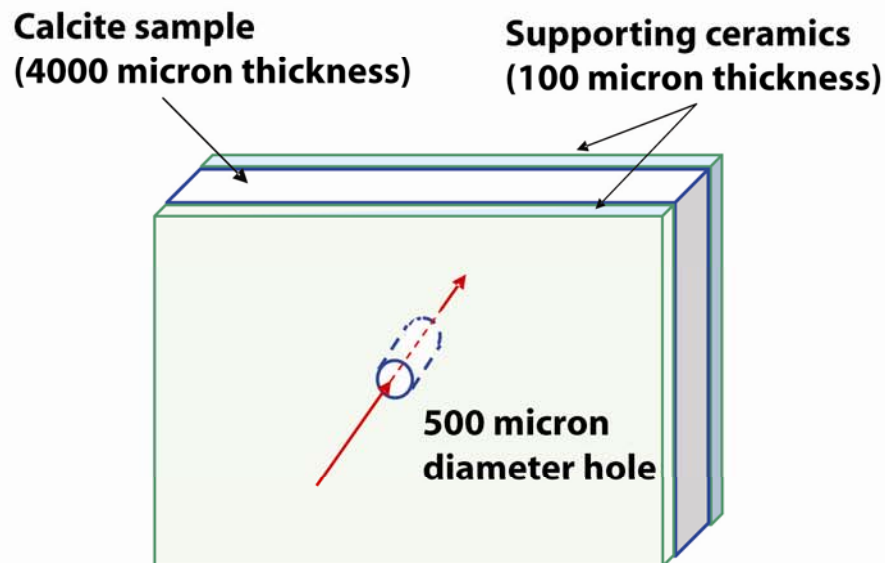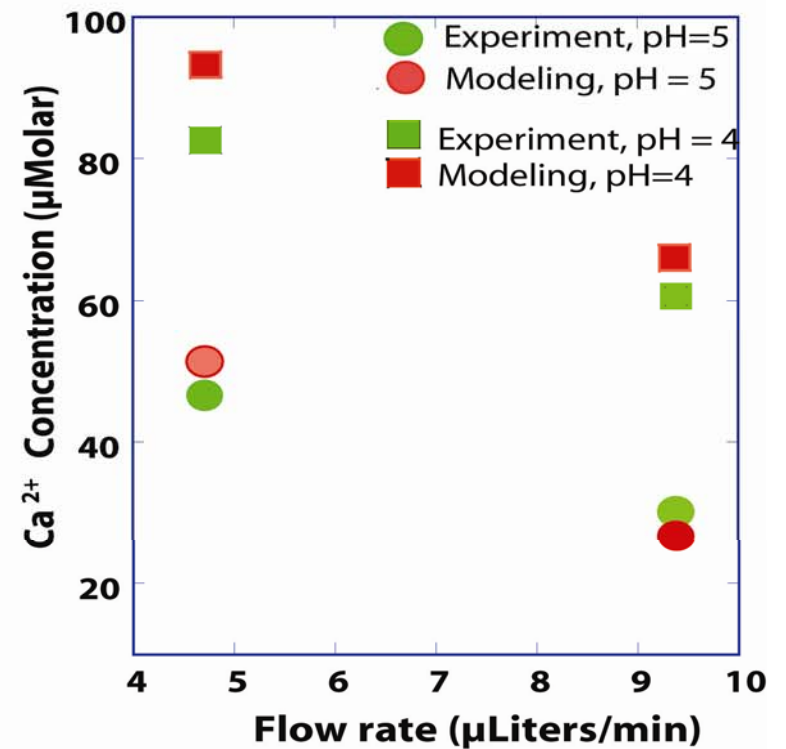
Results for a Single Calcite Pore

Compare rates from 2D reactive Poiseuille flow (R_d) with well-mixed reactor (R_m) models
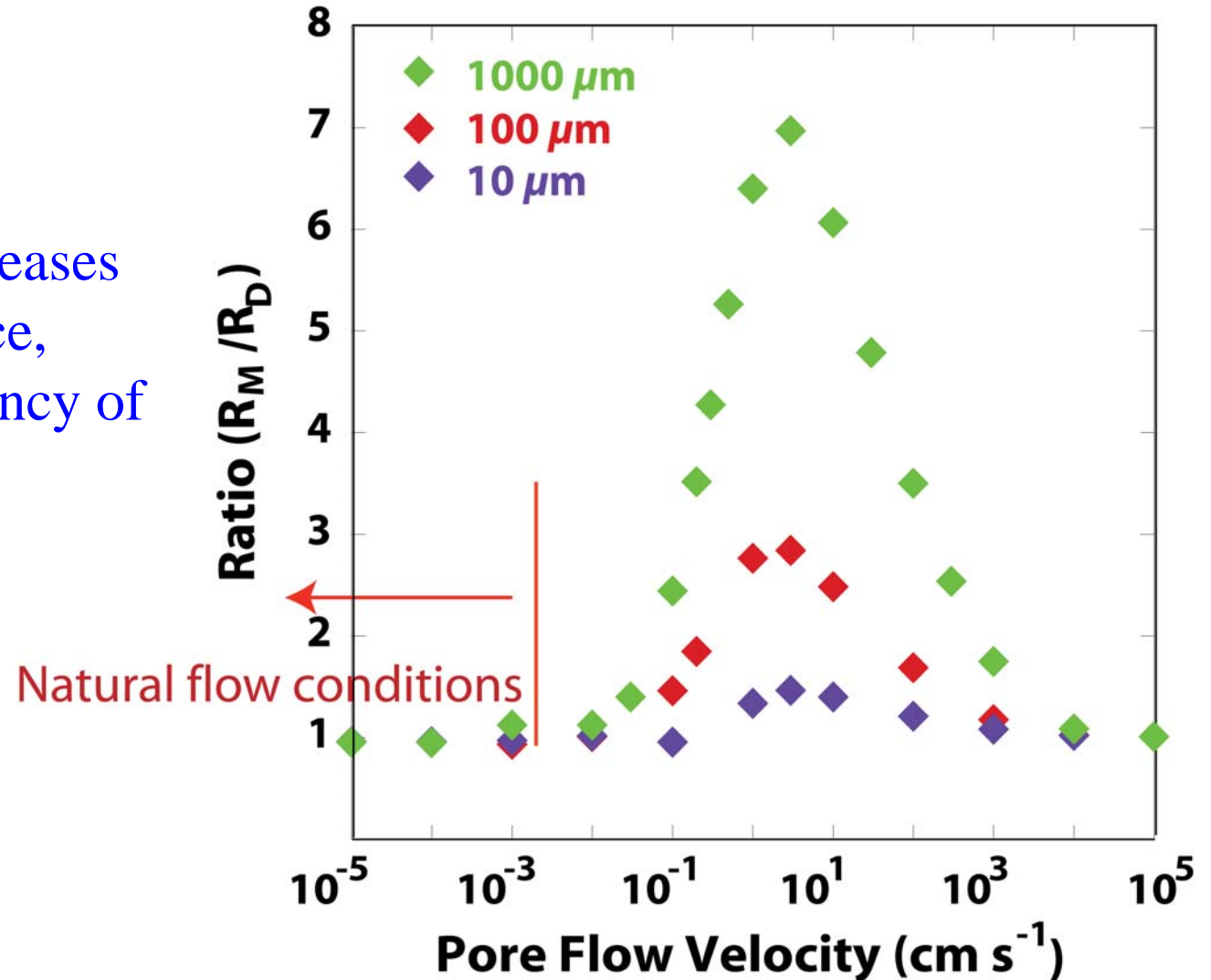
1. Transport control
   Pore fluid reaches equilibrium
2. Mixed control
   Comparable rates of flow and reaction
3. Surface reaction control
   Rates too slow relative to flow

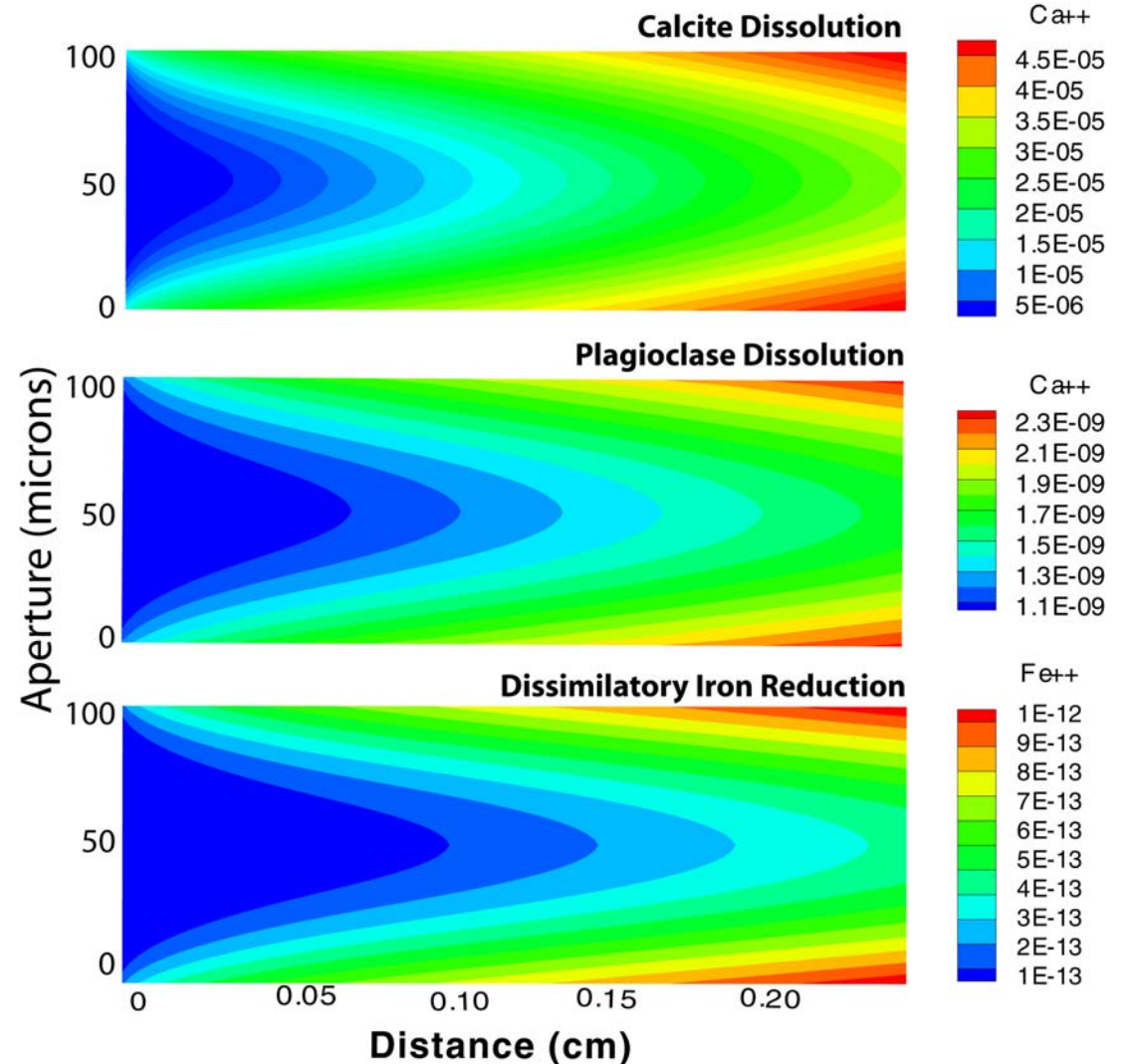# Scaling Effects as a Function of Aperture

Larger aperture increases the diffusion distance, lessening the efficiency of mixing
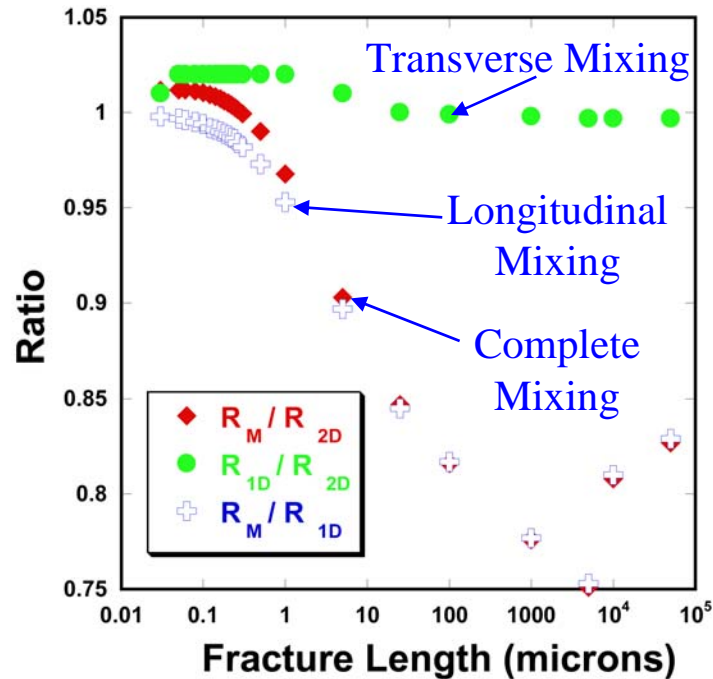
Geometry controlled by Peclet number, $Pe = v\delta/D$, but magnitude of scaling effect depends on absolute rate
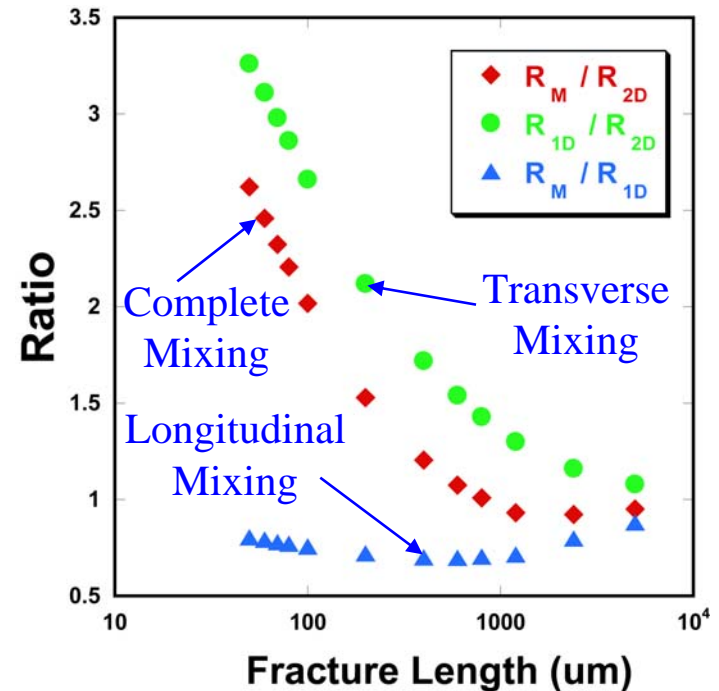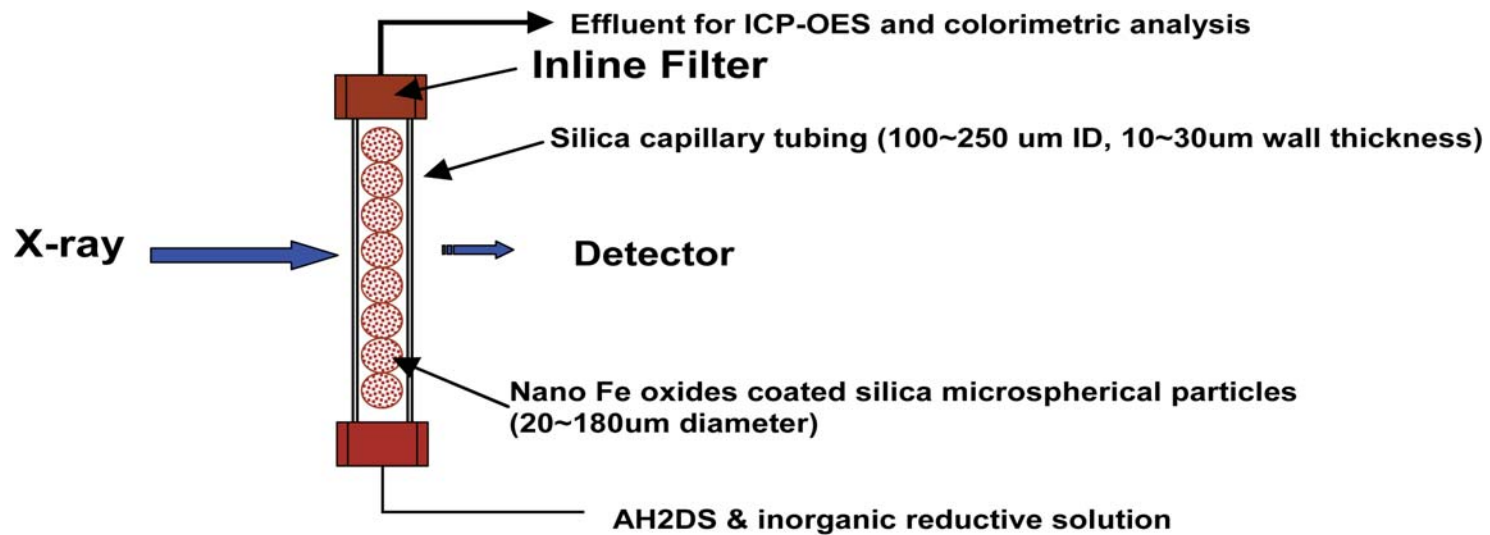
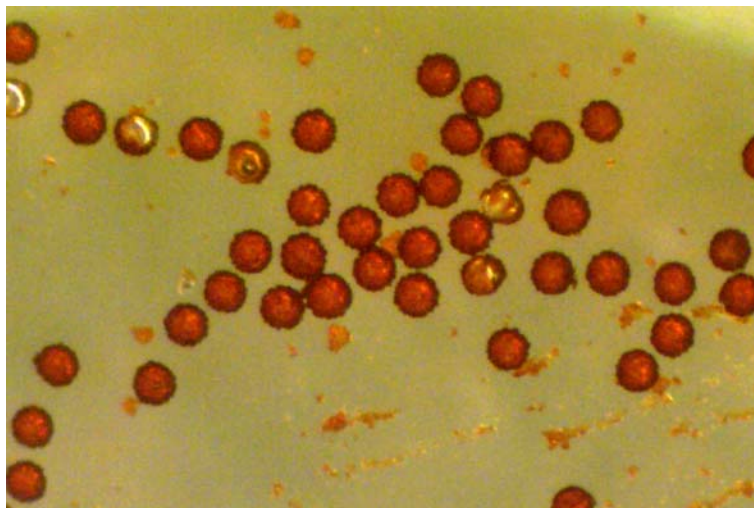# Scaling Effect as a Function of Fracture Length

Plagioclase (Al inhibition)

Calcite

Capillary Tube Experiments:
Reductive Dissolution of Fe-Hydroxide

Effluent for ICP-OES and colorimetric analysis

Inline Filter

Silica capillary tubing (100~250 um ID, 10~30um wall thickness)

X-ray → Detector

Nano Fe oxides coated silica microspherical particles (20~180um diameter)

AH2DS & inorganic reductive solution
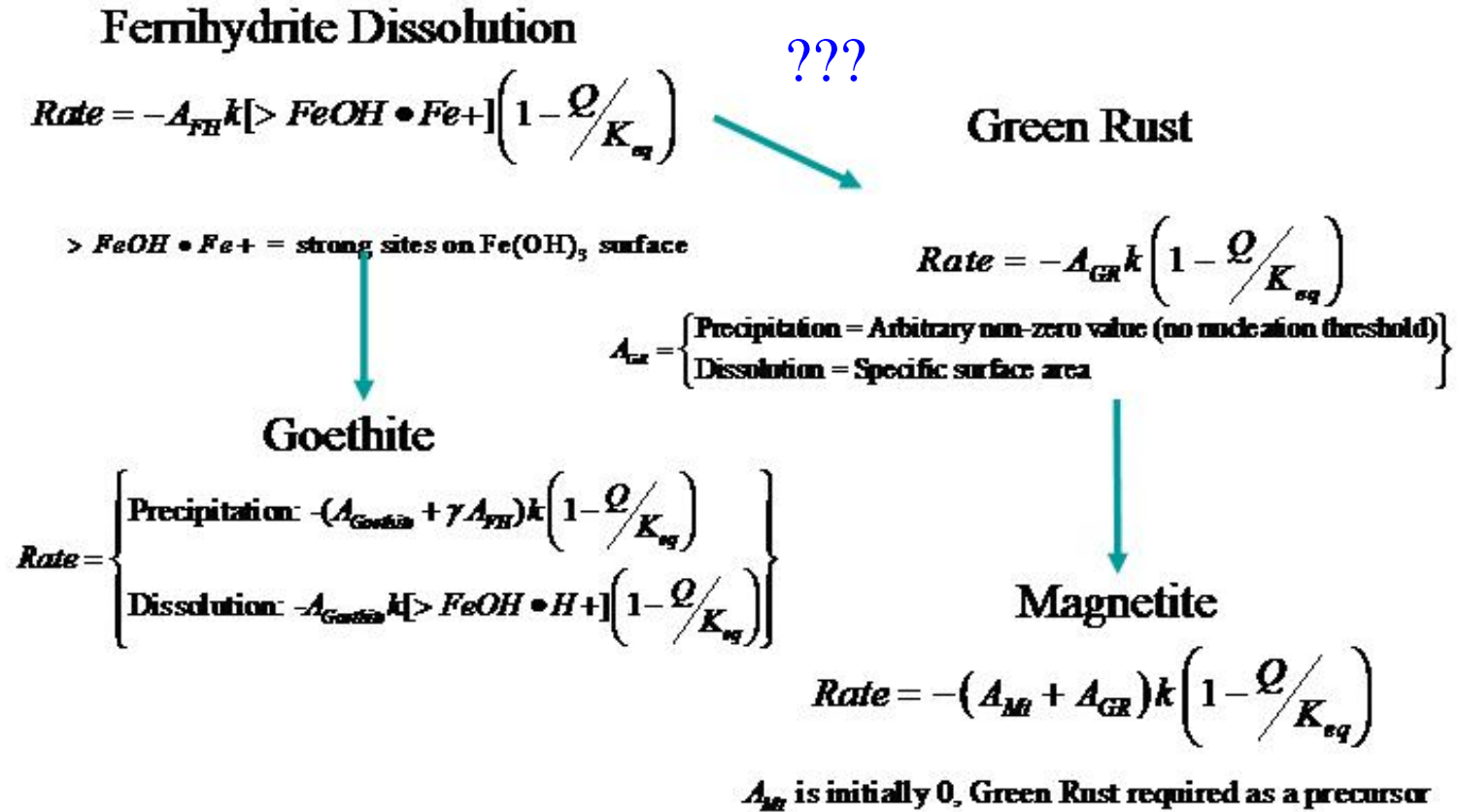
Ferrihydrite-coated glass spheres

Capillary tube with coated spheres
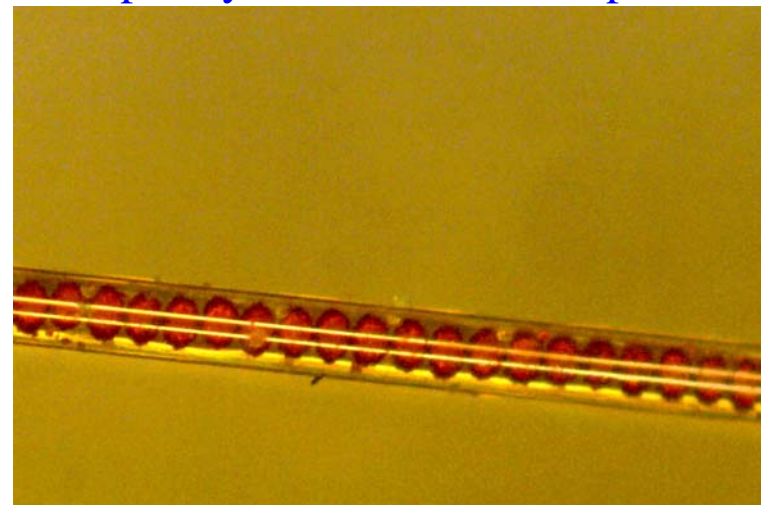
Reaction Network for Fe-Hydroxide Reduction

- Fe reduction will compete with enzymatic reduction of contaminants (U, Tc, Cr)
- Biogenic Fe can reduce some radionuclides (Tc, U?)

Ferrihydrite Dissolution

$$Rate = -A_{FH}k[> FeOH \bullet Fe+]\left(1 - \frac{Q}{K_{eq}}\right)$$

???

$> FeOH \bullet Fe+$ = strong sites on $Fe(OH)_3$ surface

Green Rust

$$Rate = -A_{GR}k\left(1 - \frac{Q}{K_{eq}}\right)$$

$$A_{GR} = \left\{ \begin{array}{l} \text{Precipitation = Arbitrary non-zero value (no nucleation threshold)} \\ \text{Dissolution = Specific surface area} \end{array} \right\}$$

Goethite

$$Rate = \left\{ \begin{array}{l} \text{Precipitation: } -(A_{Goethite} + \gamma A_{FH})k\left(1 - \frac{Q}{K_{eq}}\right) \\ \text{Dissolution: } -A_{Goethite}k[> FeOH \bullet H+]\left(1 - \frac{Q}{K_{eq}}\right) \end{array} \right\}$$

Magnetite

$$Rate = -\left(A_{Mt} + A_{GR}\right)k\left(1 - \frac{Q}{K_{eq}}\right)$$

A_{Mt} is initially 0, Green Rust required as a precursor

# Conversion of Ferrihydrite to Magnetite

- Injection of 20 mM $FeSO_4$
- Monitoring with XRD at Beamline 11.3.1 (ALS) using a 100 μm beam size
- Rate is about 1.3×10^{-10} mol/m^2/s (about 1 order of magnitude faster than reported by Hansel, Benner, and Fendorf, 2003)
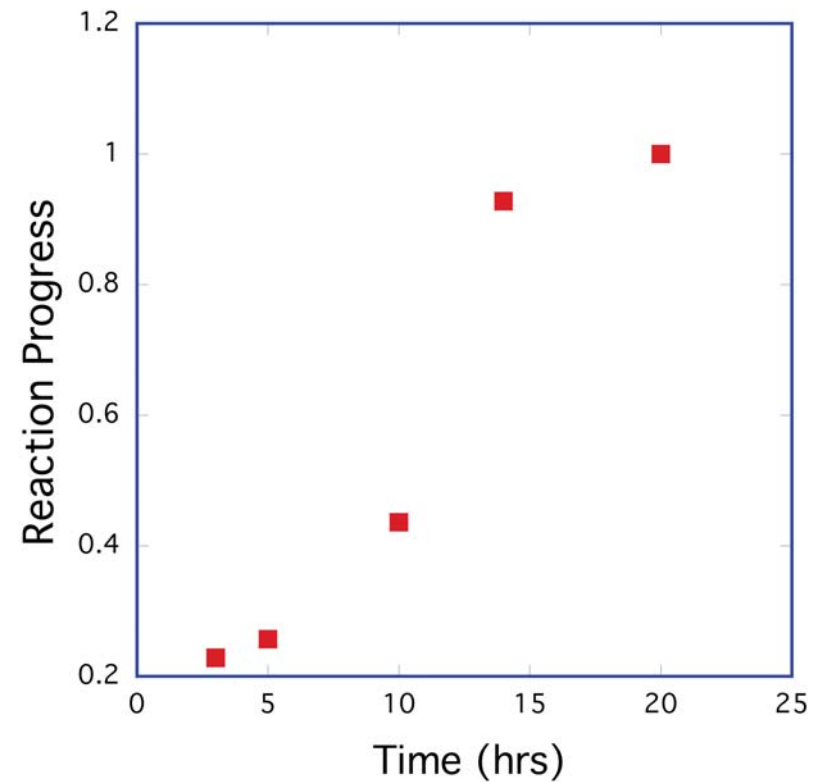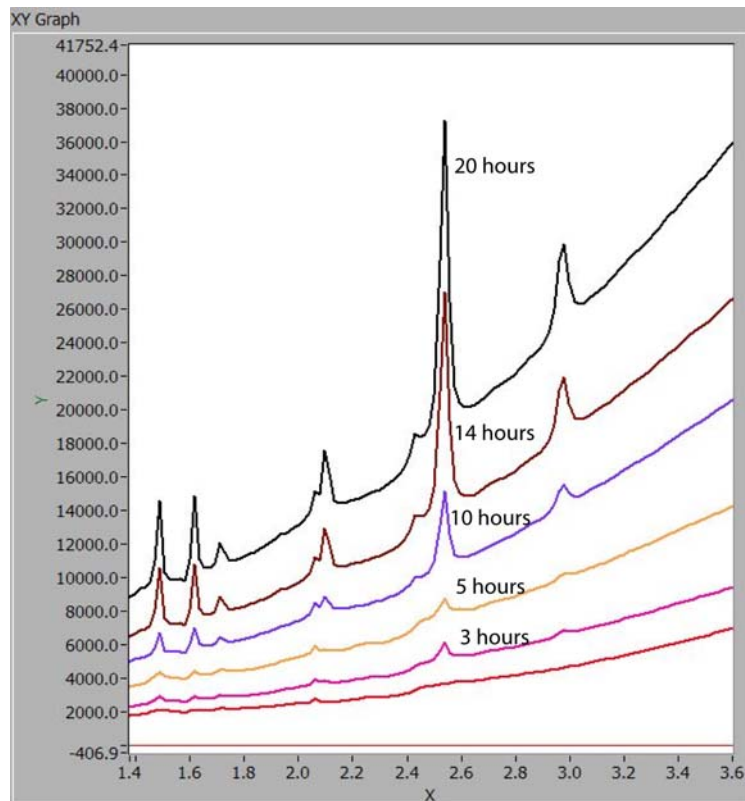
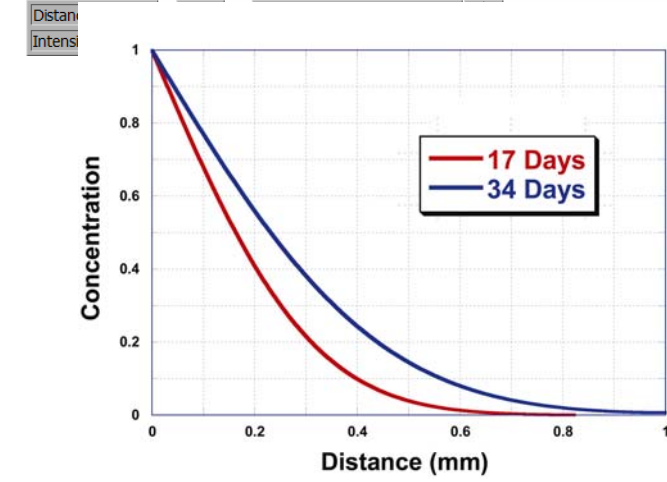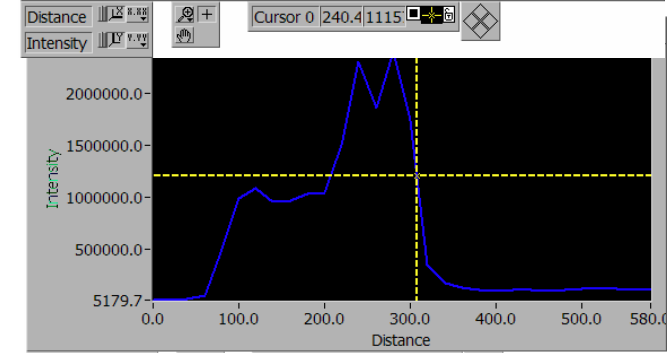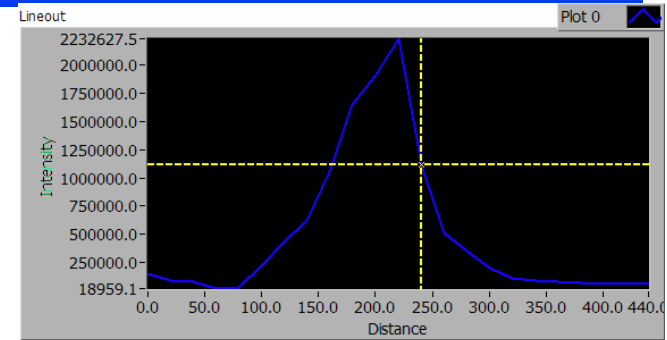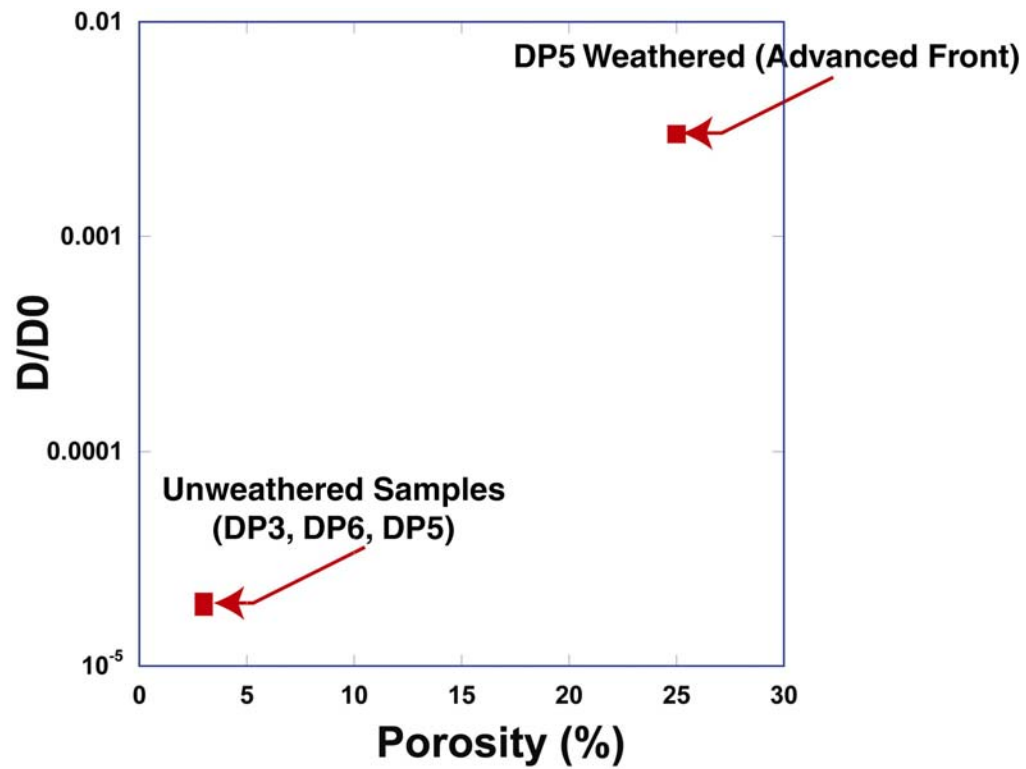# Microporosity and Diffusion Rates: Example of Weathering Rinds in Basalt
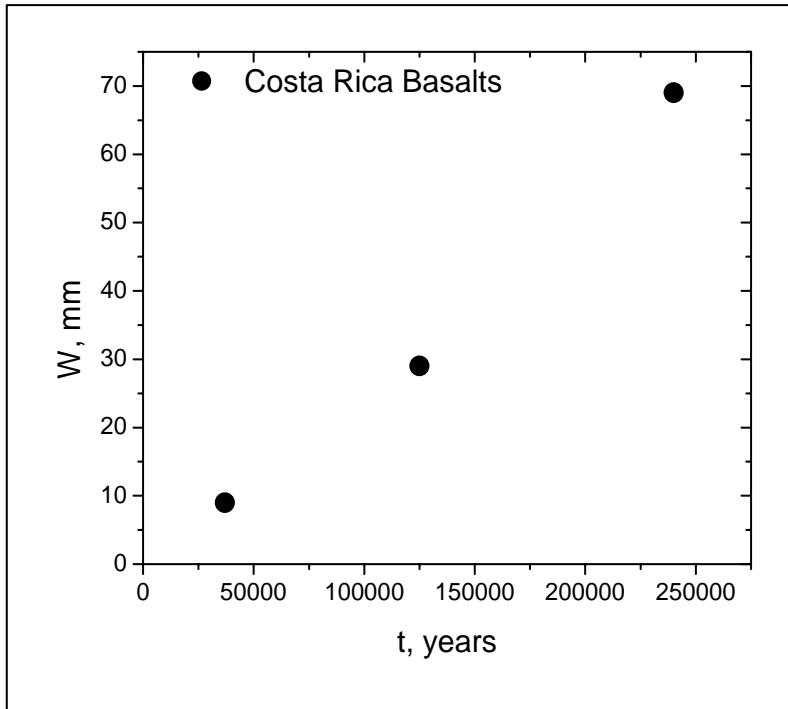
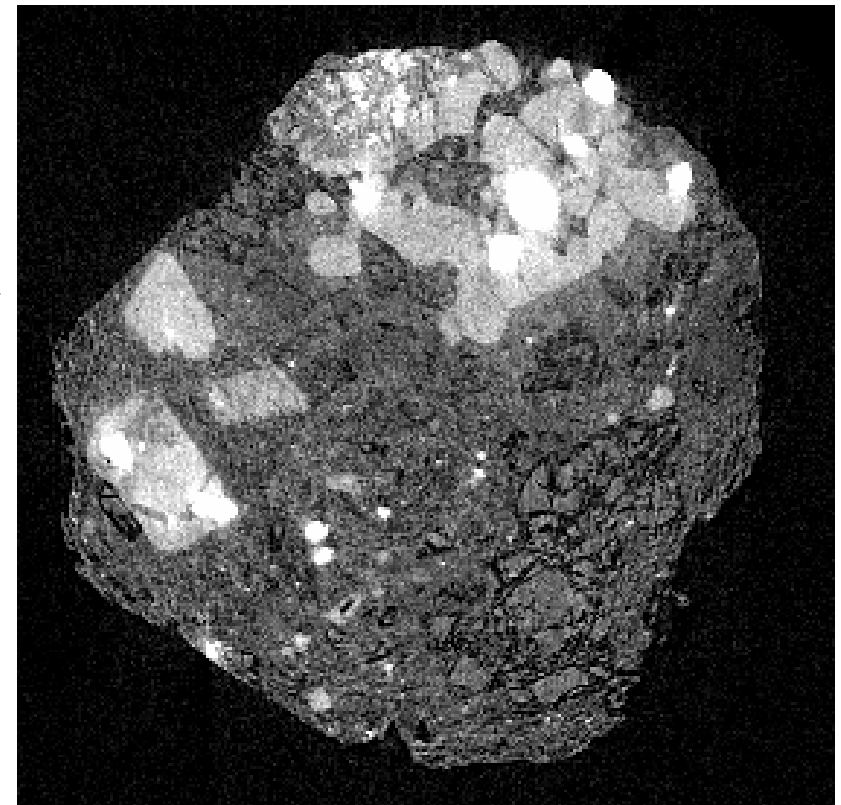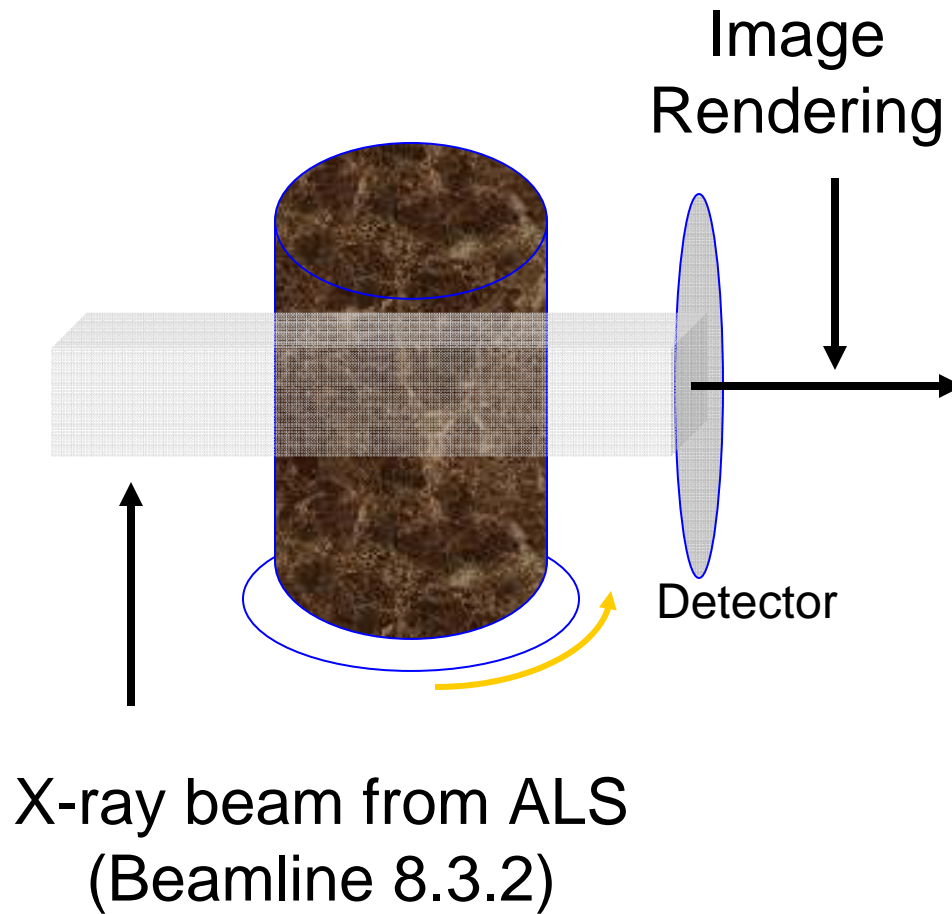**Sharp interface (< 1 mm) with porosity enhancement**
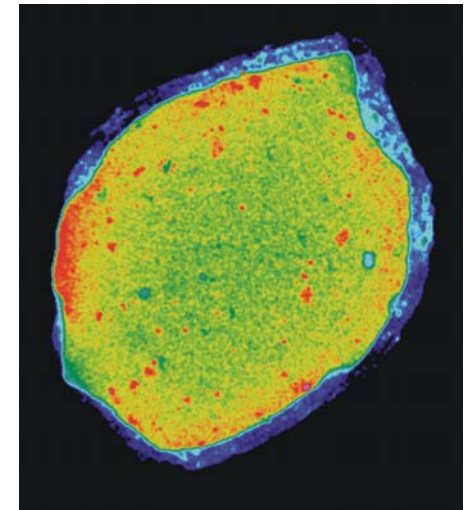
In collaboration with Alexis Navarre-Sitchler and Susan Brantley, Penn State University

μXRF Mapping of Bromide Diffusion Front

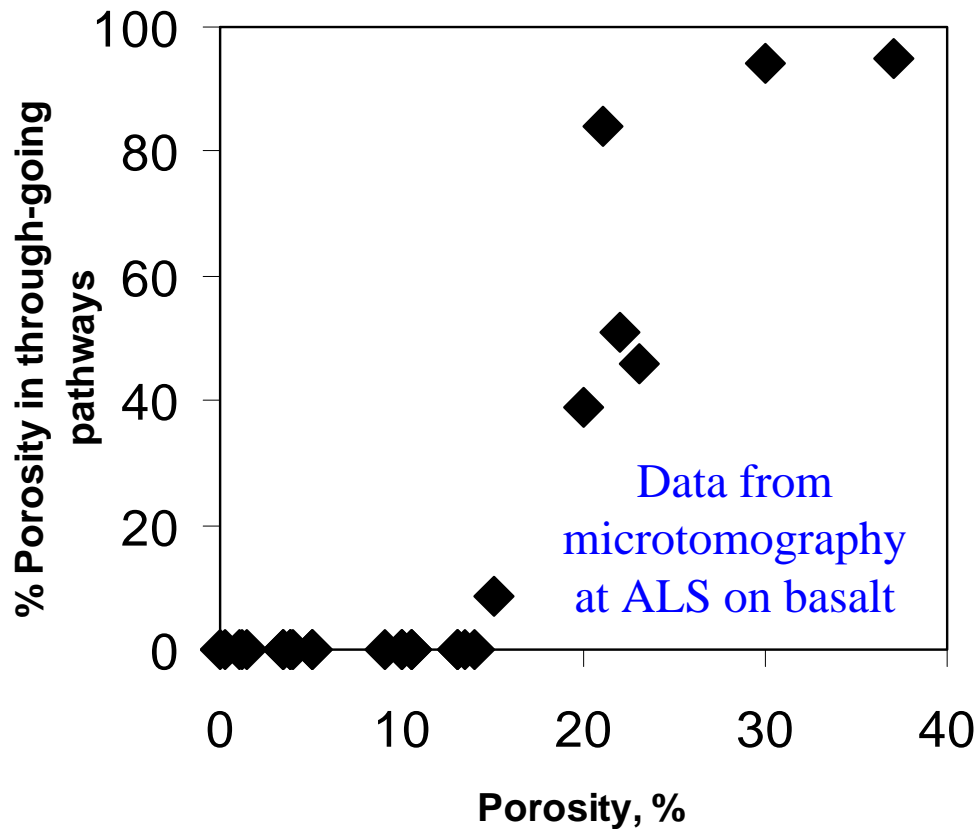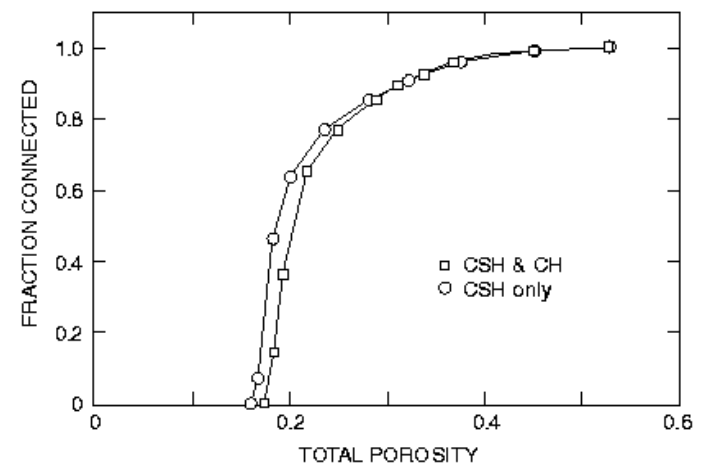# X-Ray Microtomography of Rind Interface

Image
Rendering

Detector

X-ray beam from ALS
(Beamline 8.3.2)

4.4 μm 3-D resolution

Connectivity of Porosity

% Porosity in through-going pathways vs **Porosity, %**

Data from microtomography at ALS on basalt

Connected porosity fraction calculated with "burning algorithm" in the code Percolate
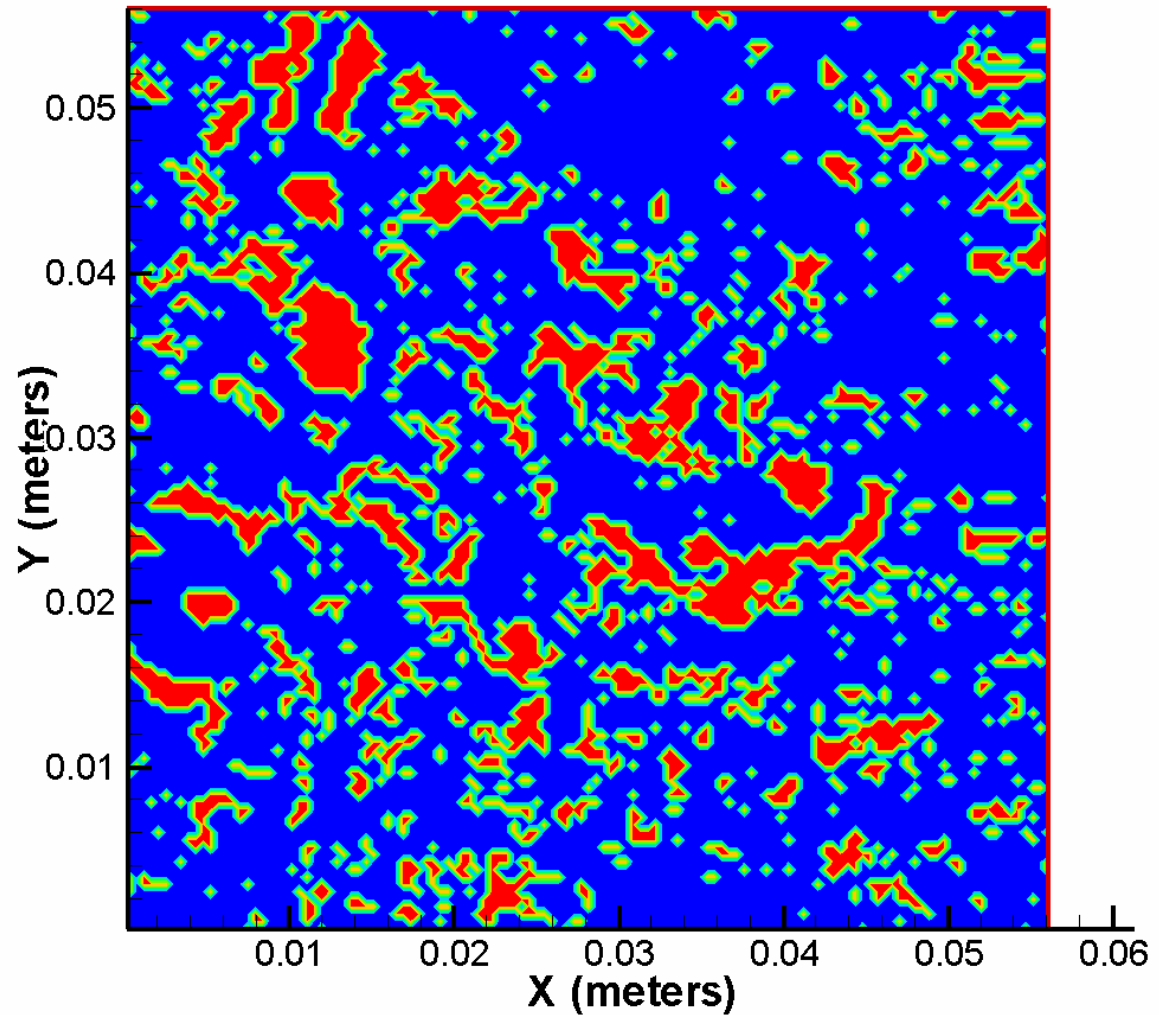

Connectivity versus porosity in cement
(Bentz, 2004)

3D Microtomography of Weathered Basalt

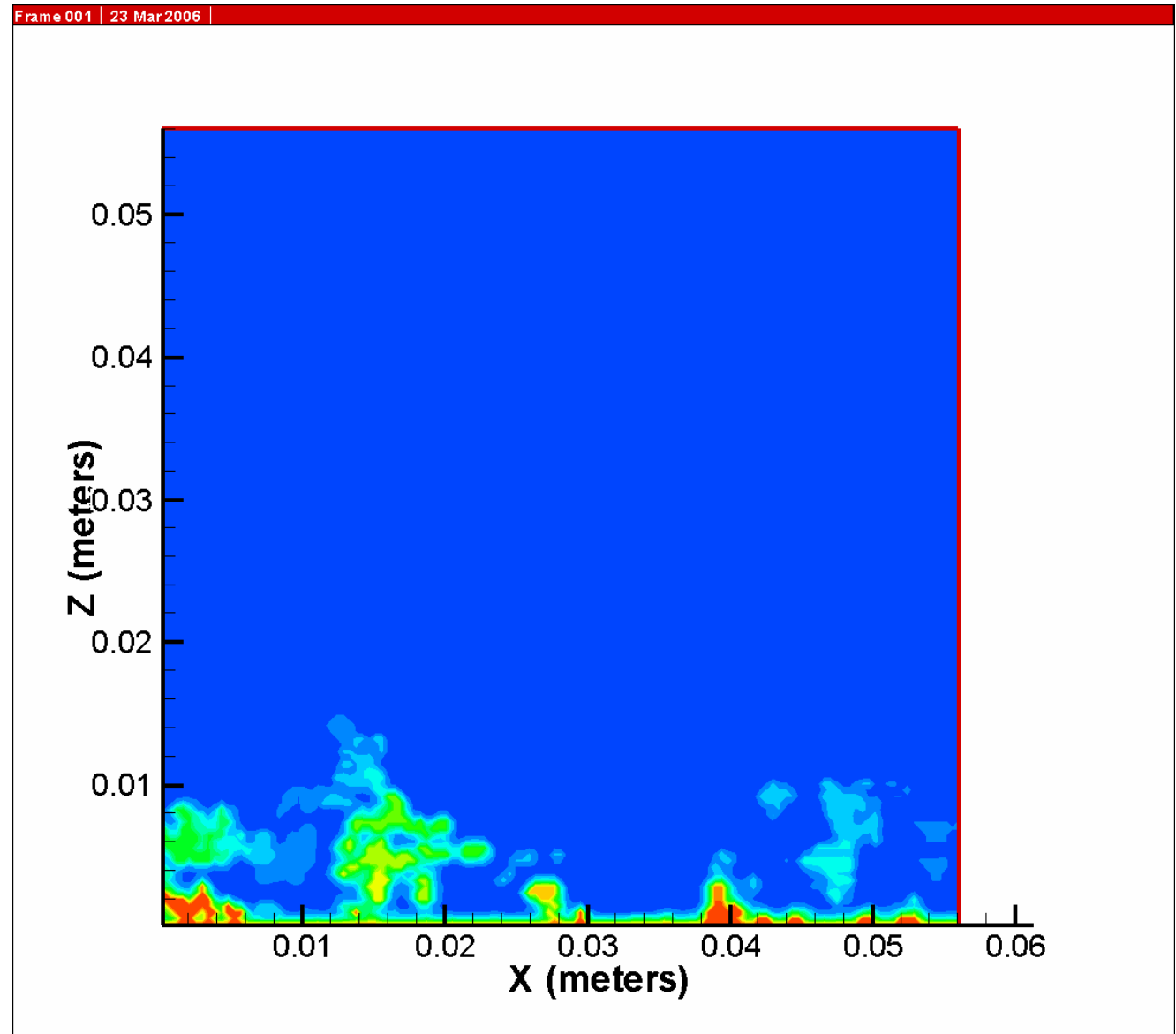Skeletonized version of 125x125x125 pixel microtomographic data
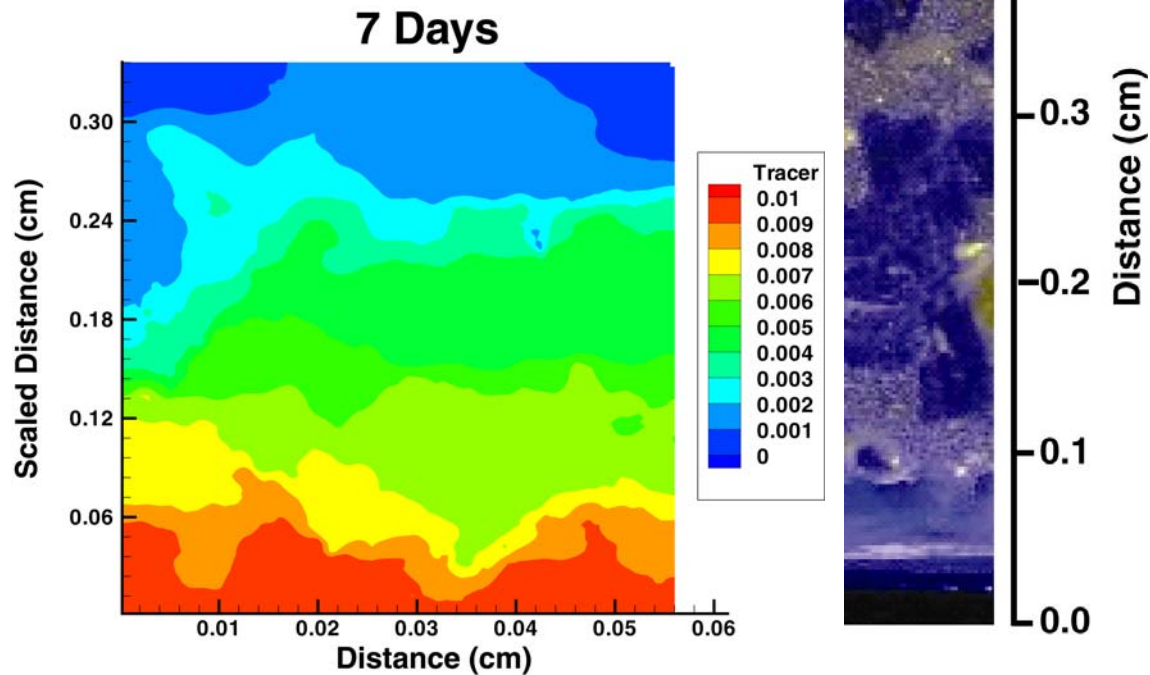- Red: Pores
- Blue: Matrix

Diffusion of a Bromide Tracer in Rind Interface

Bromide tracer released at bottom boundary, with pixel by pixel effective diffusivity based on microtomography
• Initial time: 0.001 day
• Final time: 0.2 days

Comparison of Model and Experimental Diffusion

Scaled result to 7 days assuming $t^{1/2}$ dependence
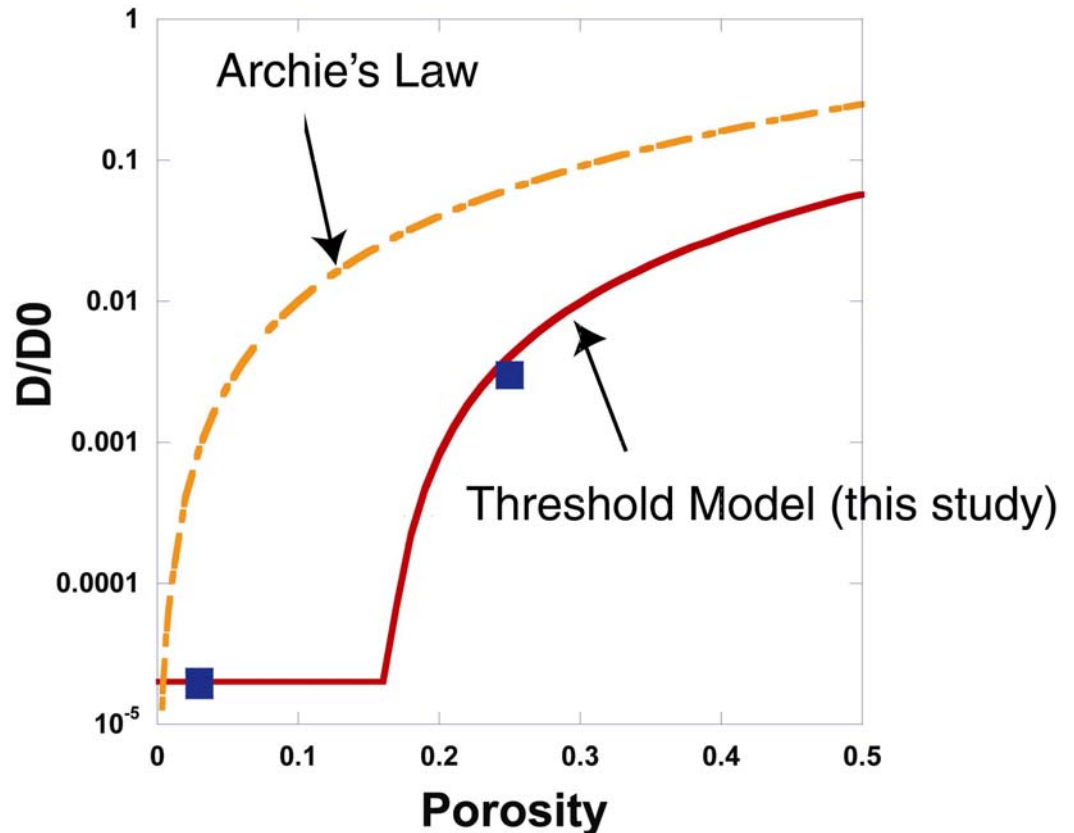
µXRF result using bromide tracer

Porosity-Effective Diffusivity Relationship

Archie's Law gives continuous increase in diffusivity with increase in porosity, even at low values

$$\frac{D}{D_0} = \phi^2$$

In **Threshold Model**, no increase in diffusivity at low porosities due to lack of connectivity

$$\frac{D}{D_0} = 2 \times 10^{-5} + 0.2 \bullet \left(\phi - \phi_{crit} \right)^2$$

Strontium Exchange in S-SX Tank Farms

- **Investigate effect of higher $NaNO_3$ concentrations on Sr exchange in sediments contaminated by tank leaks**

- **In the case of Sr (unlike Cs) the divalent cations (Ca, Mg) play a much more significant role in determining sorption, and thus retardation**

- **Dissolution and/or precipitation of calcite limits concentration range of Ca (the most important competing cation), and complicates interpretation of data**

- **Can a model be developed to capture the ionic strength dependence of the selectivity coefficients (especially Sr:Na)?**

Experimental Approach

- **Systematic batch experiments targeting pseudo-binary Ca:Sr, Ca:Mg, Na:Sr, Na:Ca (experiments by Zachara et al)**
  - Carried out at nearly constant normalities of 0.001N, 0.01N, and 0.1N
  - All relevant cations measured in pore solution and on the exchanger using ammonium chloride flush (i.e., no assumption of a binary system)

- **Column experiments using 10 μM Sr**
  - 10mM $NaNO_3$, 1mM Ca, 1mM Mg
  - 100mM $NaNO_3$, 1mM Ca, 1mM Mg
  - 100mM $NaNO_3$, 0.5mM Ca, 0.01mM Mg
  - 30mM $NaNO_3$, 0.5mM Ca, 0.01mM Mg

Modeling Approach

- **Compare and contrast single-site and multi-site models**

- **Evaluate the possibility that exchange of monovalent ion pairs ($SrNO_3^+$, $CaNO_3^+$, $MgNO_3^+$) occurs, accounting for the relatively stronger sorption of divalent cations at high Na concentration**

- **Inclusion of carbonate dissolution and precipitation**

- **Reconcile (if possible/necessary) the batch and column experiments**

Two-Site Model for Exchange in Batch Experiments
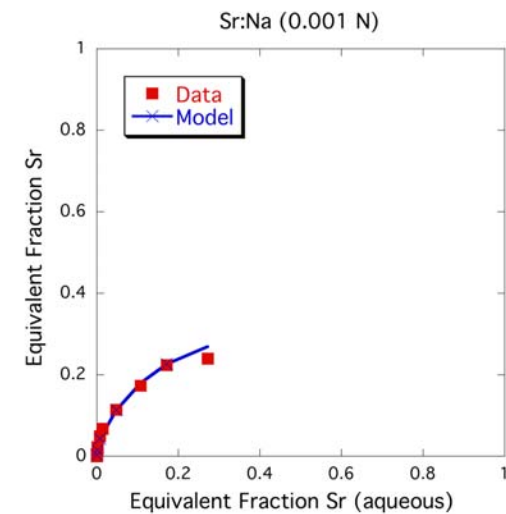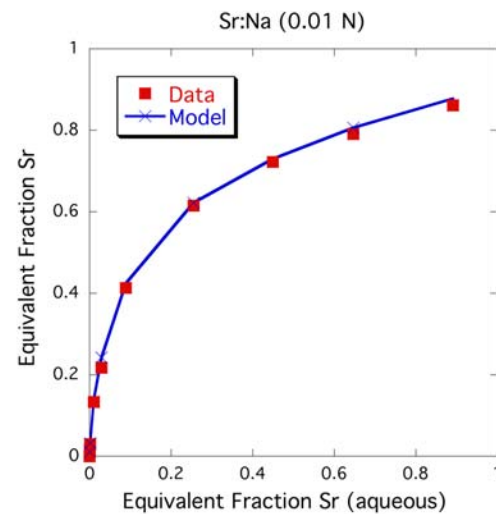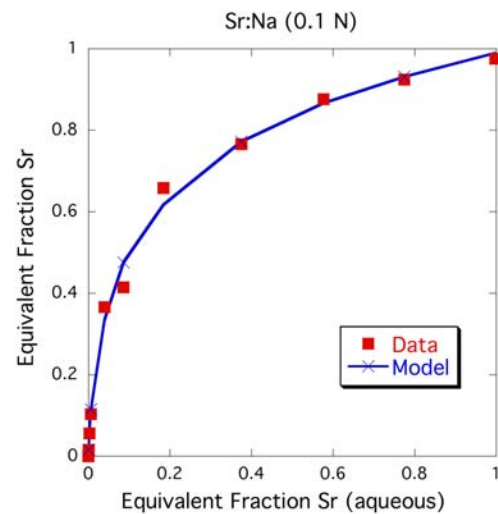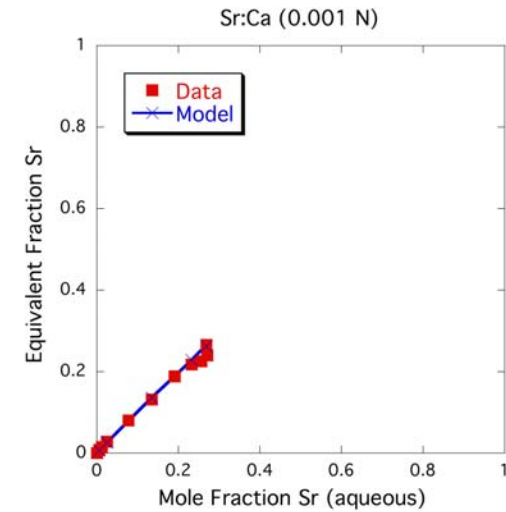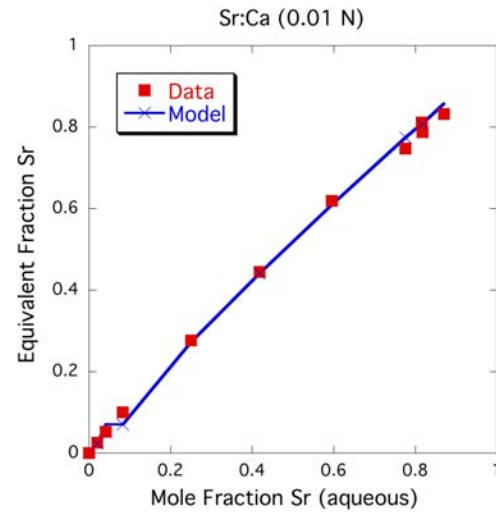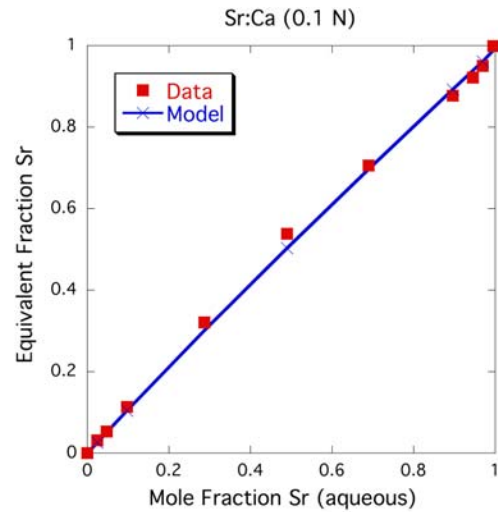
Exchange Involving Monovalent Ion Pairs?

Can the apparent ionic strength dependence of selectivity coefficients be explained with monovalent ion pairs?
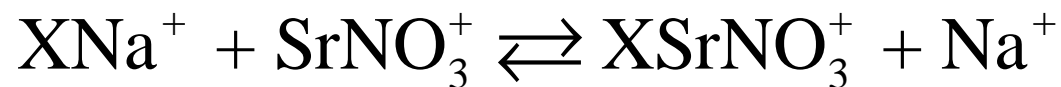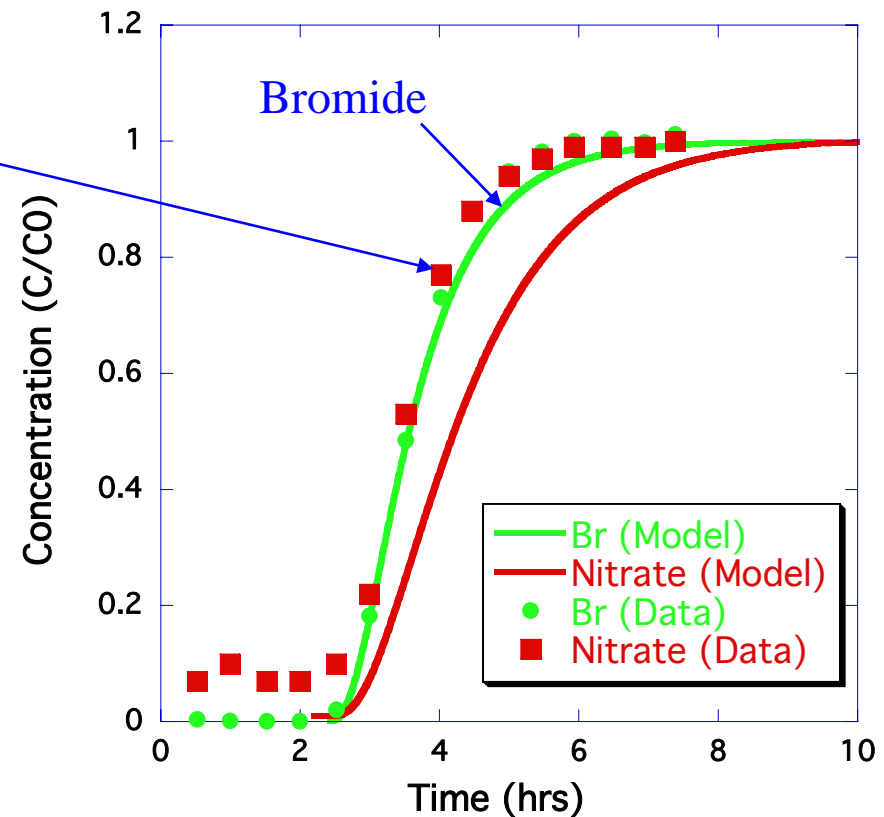
$$XNa^+ + SrNO_3^+ \rightleftarrows XSrNO_3^+ + Na^+$$

Fit of batch data using exchange of monovalent ion pairs predicts substantial retardation of nitrate breakthrough
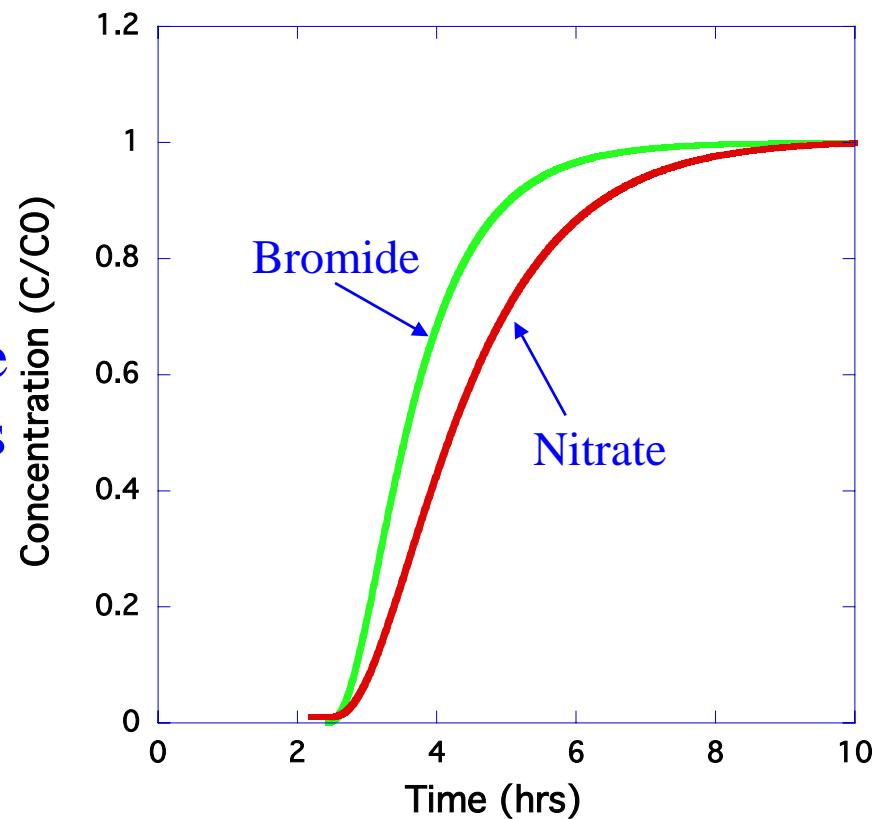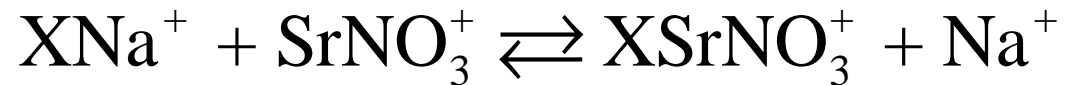
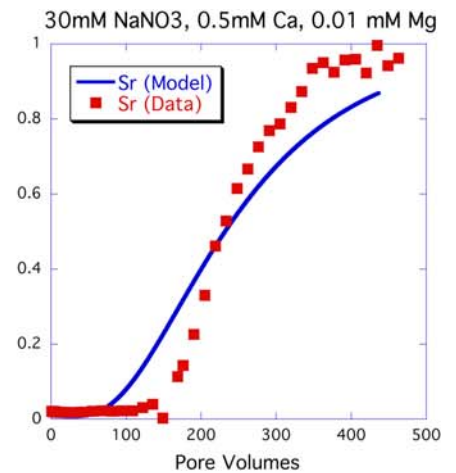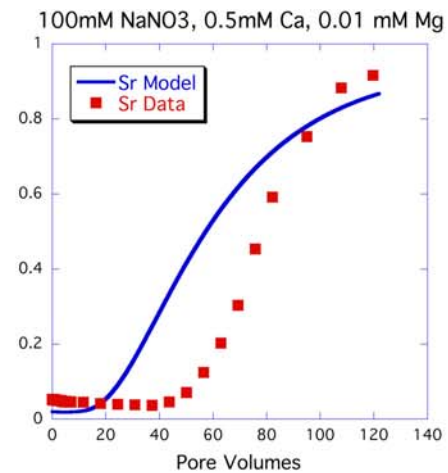# Exchange Involving Monovalent Ion Pairs?

No retardation of nitrate observed

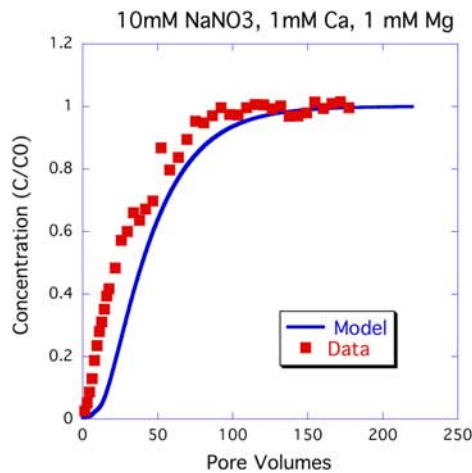
$$XNa^+ + SrNO_3^+ \rightleftarrows XSrNO_3^+ + Na^+$$

Selectivity Coefficients from Batch Experiments

|	Log Na/Sr	Log Na/Ca	Log Na/Mg
Site 1 (58%)	0.00	-0.01	-0.11
Site 2 (42%)	-1.37	-1.19	-0.64
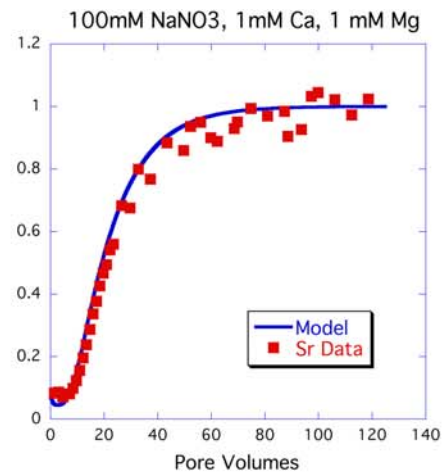
Sr Transport at Hanford 100N

■ **Strontium contamination near the Columbia River involves seasonal oscillation in groundwater wells**

  ↗ **Increase in river stage causes intrusion of dilute Columbia River water**

  ↗ **Lowering of river stage results in return of more concentrated (Ca, Na, Mg) groundwater (although still dilute compared to the Hanford tanks)**
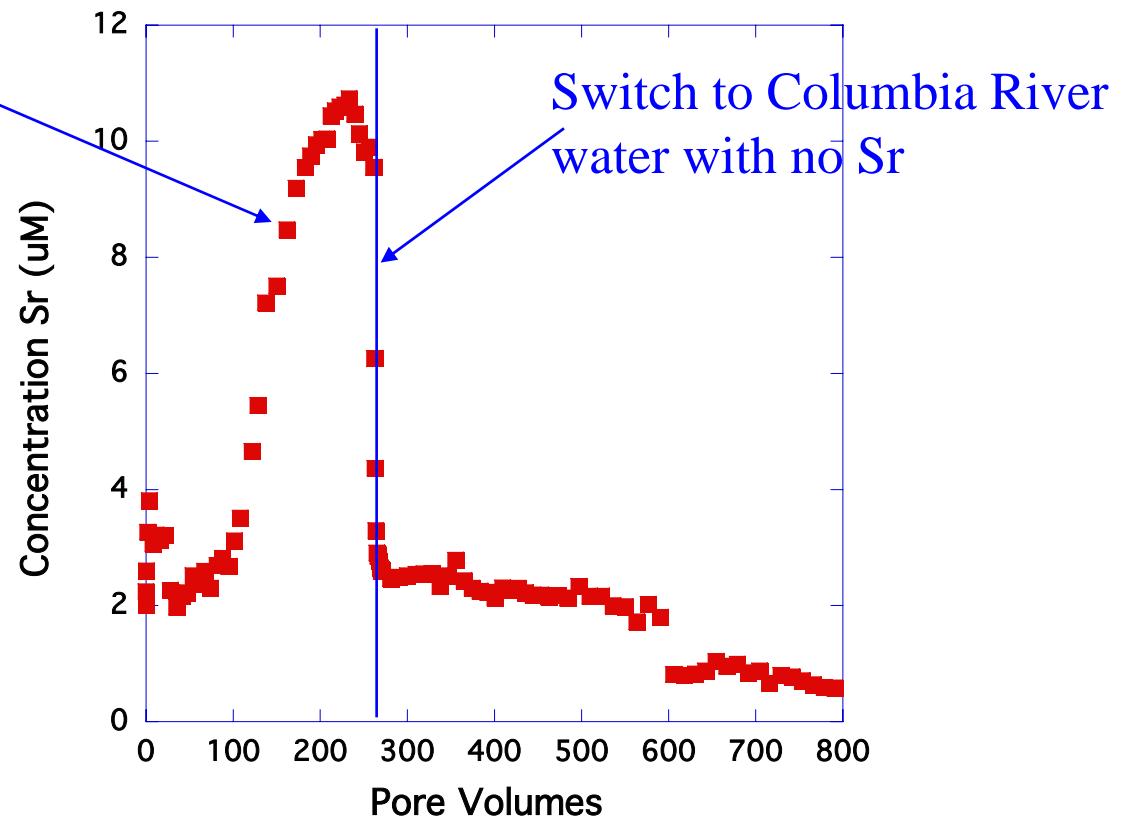
Hanford 100N
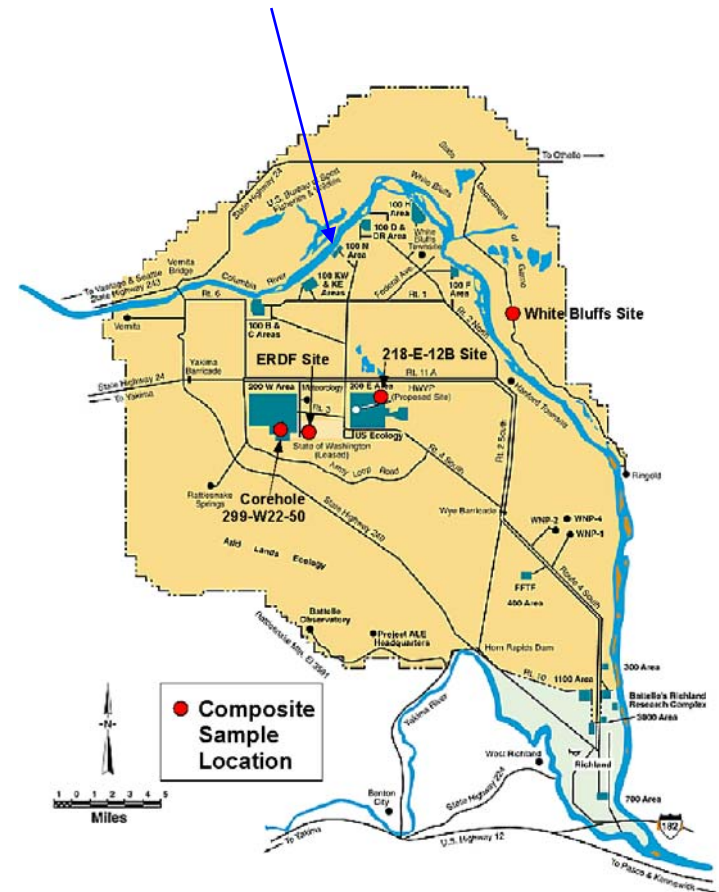
Exchange and Transport at Hanford 100N

Elution of 10 µM Sr in "groundwater" matrix

Switch to Columbia River water with no Sr

Summary and Conclusions

- **Scaling effects for reaction rates at the pore scale are minor (at best) due to**
  1. **Efficiency of diffusive mixing**
  2. **Slowness of many rates in the subsurface**

- **Upscaling of rates necessary at larger scales where mixing via diffusion is incomplete (pore network and >)**

- **Capillary tube experiments ideal for combining simultaneous measurement of solid-solid transformation(s) and effluent chemistry**

- **X-ray microtomography offers promise for improving estimates of diffusivity and reactive surface area**

- **The K_d for Sr is quite sensitive to relatively small changes in groundwater chemistry (especially Ca)-- Role of ion pairs ($SrNO_3^+$) is minor**